The clinical implications of computerised fluid dynamic modelling in rhinology*

Sandro H. P. Leite, Ravi Jain, Richard G. Douglas

Department of Surgery, The University of Auckland, Auckland, New Zealand

Rhinology 57: 1, 2 - 9, 2019
https://doi.org/10.4193/Rhin18.035

***Received for publication:**
February 18, 2018
Accepted: June 25, 2018

Background: The nose is a dynamic organ and is the first point of contact between inhaled air and mucosal surfaces. Within the nasal cavity, there are changes of air flow and pressure occurring during the respiratory cycle, as well as exchanges of heat and humidity, and important immune responses to inhaled antigens and allergens.

Methodology: This review is a summary for rhinologists covering what is known about airflow within the nose and sinuses and the impact of pathology and treatments on the physical environment of the nasal cavity. The review will concentrate largely on the significant contribution that computational fluid dynamics has had on this field.

Results: The complex anatomical structure of the nasal cavity provides an aerodynamic environment that guides the airflow throughout the nasal cavities. However, anatomical or inflammatory changes can modify the air flow, heat and humidity exchanges, with negative consequences on nasal physiology. Restoration of normal airflow is a key goal to achieve success in the treatment of nasal diseases.

Conclusions: Computational fluid dynamics is a method of analysis originating from engineering which has been adapted for rhinology. Although still an expensive and laborious technique, it may become a viable diagnostic tool in the future for studying nasal physiology.

Key words: computerized models, computer simulation, fluid dynamics, nasal cavity, paranasal sinuses

Introduction

Many different methods have been developed to determine airflow and other variables in the nasal cavity. However, each of these has been hampered by the complexity of the nasal anatomy and the difficulty of inserting sensors into the nasal cavity without changing its physiology [1].

There are currently three physical techniques in common use. Rhinomanometry measures pressure and airflow during respiration to define the resistance of the nasal airway. Acoustic rhinometry uses the sound waves reflected from the nasal walls to create a two-dimensional image of the nasal cavity [2]. These tests have significant limitations since they do not show the entire nasal function, such as local flow and pressure changes, turbulence, and heat exchanges [3]. The measurement of peak nasal inspiratory flow (PNIF) is a validated technique that has been shown to be valuable as an objective assessment of nasal patency [4]. It has been used to analyse nasal airflow in respiratory diseases as well as to evaluate results of clinical or surgical treatments [5, 6]. However, this method has limitations because it is dependent on lung function, body position, and the cooperation of the individual tested [7, 8]. Therefore, a better way of visualising the complexity of nasal airflow is required.

Computational fluid dynamics (CFD) is a discipline derived from the union of fluid mechanics, mathematics and computer science, which uses numerical simulations to analyse data related to interactions of liquids, particles or gases whose motion is limited by solid surfaces, as well as to evaluate heat or humidity exchange across surfaces [9, 10]. The study of fluid dynamics simulating airflow in the nasal cavity was initially performed using anatomic plastic models [11]. The first anatomically accurate

3-D computer-generated model of airflow in the nose based on CT scan results was described in 1995 [12]. Since this time CFD modelling has been used to study airflow, heat and humidity exchanges, as well as topical delivery of drugs into the nasal cavity and paranasal sinuses under normal or pathological conditions. In this review, we will describe the contributions of CFD to clinical rhinology, as well as review the studies which validate this method.

Methods

The studies analysed were obtained from an online survey on the database of the University of Auckland (New Zealand), the US National Library of Medicine (PubMed), MEDLINE (Ovid), Google scholar, ClinicalKey and Cochrane Library. A combination of MeSH key terms (rhinology, nasal cavity, paranasal sinuses, fluid dynamics, computerized models, computer simulation, physiology, and surgery) and non-MeSH terms (computational fluid dynamics, CFD, numerical simulation, airflow, particle deposition, thermal exchange, humidity exchange, validation, and model development). A time-out filter was applied for articles published after 2004. Articles prior to this period were cited only as historical references. All manuscripts were analysed for use of CFD in rhinology.

Results

Model development

The first step to creating a three-dimensional model of the nasal cavity and paranasal sinuses is the acquisition of data from a computerized tomography (CT) scan or a magnetic resonance image (MRI) of the nose and paranasal sinus [13]. The slice thickness of the exam impacts on the quality and resolution of the reconstruction in three dimensions. Resolutions of 1 mm are acceptable to study the nasal cavity, although higher resolutions are optimal if the study is focused on paranasal sinuses [14]. After the data set is acquired, the images need to be processed in order to be converted into a 3-D computational model (Figure 1)[15]. For this propose, the images need to be subjected to the processes of filtration, segmentation, surface reconstruction and mesh generation [16].

After obtaining a 3-D model of the nose and paranasal sinuses, software that uses equations based on the conservation laws of physics are applied to these models to simulate numerically the inspiratory and expiratory airflow [10], and to derive laminar or turbulent airflow patterns, heat or humidity exchange, and particle deposition [17] (Figure 2)[15].

CFD is a demanding process, taking several hours of work by a specialist bioengineer and a high-performance computer to perform only one simulation [9, 16]. However, the amount of information obtained from these studies has greatly contributed to increased knowledge about the physiology of the nose and paranasal sinuses and some of these contributions will be described below.

Airflow

Before the development of CFD techniques in otolaryngology, it was difficult to describe the variations in air flow within the nasal cavity and paranasal sinuses using human or "nose like" models [14, 18, 19] since techniques that require equipment or sensors placed in the nasal cavity may disturb the normal airflow. Although cadaver-based models are easier to create, postmortem tissue shrinkage can distort the nasal airway's anatomy [20]. The development of CFD techniques has allowed the simulation and visualization of airflow patterns in the entire nasal cavity and paranasal sinuses in health or disease [9, 21], improving the understanding of the nasal physiology as well as the planning of surgical treatments [3].

CFD has been used to analyse the airflow in 20 adult healthy noses [19] and found the flow accelerated in the nasal valve region, due to the resistance in this region, slowed posteriorly in the nasal cavity and increased again in the nasopharynx. Only a small proportion of streamlines were found in lower nasal meatus. Most of the flow went through the lower part of the olfactory cleft and middle meatus. These findings have been confirmed by others who found that nasal resistance and shear stress on the wall reached a peak in the region of the nasal valve [22], and the values of nasal resistance measured by rhinomanometry were similar to those found using CFD [23].

In a normal nasal cavity, CFD models also demonstrate that the airflow follows three distinct paths. The first stream originates on the edge of the nostril and goes dorsally to the region of the olfactory cleft, the second comes from the central portion of the nostrils and goes to the middle meatus, and a third flow goes to the inferior meatus, originating from the base of the nostrils [24]. These simulations have demonstrated that in a healthy nose the main airflow is located between the inferior and middle turbinates [25]. However, with a septal deviation, this flow is more complex, passing through the floor and the roof on the side of the deviation, and with an increase in its velocity. CFD has shown that the nasal valve region is the area where the most turbulent flow occurs. In septal deviation, this phenomenon is reduced or even disappears, particularly if the deviation is located close to the nasal valve [25, 26]. These findings are similar to cases of hypertrophy of inferior turbinates with severe obstruction, where the influence of the nasal valve virtually disappears [18]. Measurements on synthetic models using particle image velocimetry confirm the relationship between nasal geometry and airflow and can validate the CFD results [27].

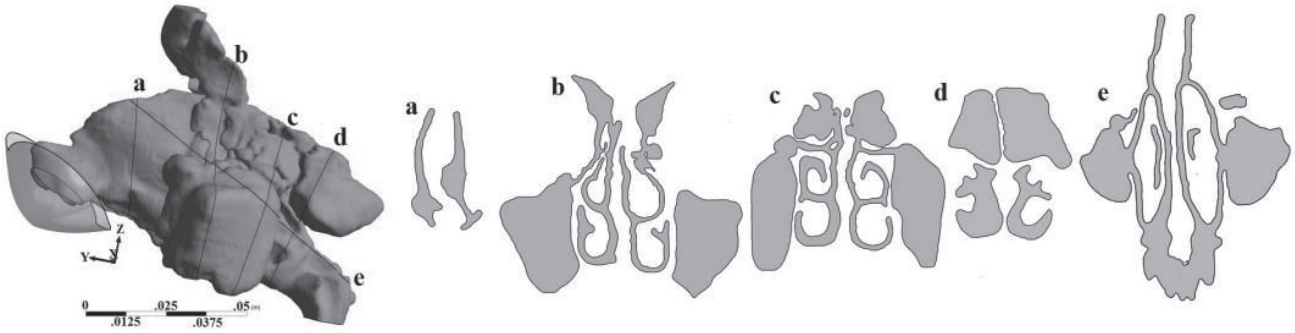

Figure 1. 3D nasal cavity geometry of a healthy normal subject and cross-sectional views of the nasal airway. Retrieved from Kumar et al. [15].

CFD modelling has been used to predict changes in airflow in surgical situations and showed that aggressive sinus surgery that considerably enlarges the nasal cavity reduces the contact between airflow and the nasal wall, and resultant air conditioning [28]. Others have found variations of airflow, pressure, velocity, temperature, nasal resistance, and heat exchange following various degrees of middle or inferior turbinate resection [13, 29]. These changes were more prominent in near total resection models.

CFD virtual surgery can be performed to predict the physiological outcomes and improve the success rate after real surgical procedures. Virtual septoplasty and partial lateral turbinectomy to treat nasal obstruction have been simulated and demonstrated an airflow increasing through the middle meatus and a general reduction in the intranasal airspeed [30]. Different turbinectomy techniques have been simulated using CFD and showed a reduction of airflow near the olfactory region when the head or almost all the inferior turbinate were resected, which could reduce the sense of smell in the postoperative period [31]. The excision of the lower fifth of the inferior turbinate did not change this flow. Using CFD, new techniques such as pyriform turbinoplasty and nasal wall lateralization have shown an increase in the airflow as a strategy to open the nasal valve to treat nasal obstruction preserving the turbinates [32]. Thus CFD may be useful to demonstrate the effects of turbinate enlargement and to test new surgical strategies for optimizing airflow [21].

From a sinus surgery perspective, CFD has also been used to quantify the improvement in paranasal sinuses ventilation. It has been shown that the airflow into maxillary sinus was virtually zero before surgery [33, 34]. However, after performing different sizes of virtual antrostomy, the airflow increased between 0.2% to 50.5%, depending on the antrostomy size. The average airflow has been shown to increase into the maxillary sinus by 18.5mL/s (5.2 - 28.2 mL/s) after functional endoscopic sinus surgery (FESS) where the size of the maxillary ostium was enlarged to about 122.9 mm^2 (101.9 mm^2-151.2 mm^2) [35]. Airflow also increased remarkably in the maxillary sinus after uncinectomy and middle meatal antrostomy, from 1% in a normal nose to about 25% after the surgery [36]. These CFD data suggest a close relationship between the size of the post-op maxillary ostium and the increase of airflow into this sinus. Similarly, virtual sphenoidotomy has been shown to increase considerably the airflow into the sphenoid sinus [37] since about only 0.013% of the inhaled air reaches the sphenoid sinus preoperatively, increasing to 17% after surgery.

One of the major challenges related to airflow study and CFD is whether the results can be validated by other measurements. The results of airflow measurements between CFD simulations and anterior rhinomanometry in a similar mucosal condition have been compared and found to be very similar [38]. Models can also be useful to validate the CFD simulations. 3D-plastic models have been built to study airflow patterns through the nasal cavity by flow visualization and particle image velocimetry, and the results have shown different airflows in each nasal region [39]. The slower flow in the olfactory region, more rapid and unstable flow in the turbinate region and a laminar flow mainly passing through the middle meatus corroborate well with CFD simulations [40].

Thermal and humidity exchange

Both temperature and humidity rise as inhaled air passes through the nasal cavity mostly at the anterior third of the nasal airway [41]. Miniaturized thermocouples on the nasal mucosa have shown that during inspiration, air temperature declined from 32.5°C to 30.2°C in the region of nasal valve, and from 34.4°C to 33.2°in the nasopharynx [42]. However, the complexity of the nasal anatomy hampers direct measurement and the insertion of probes and sensors may cause perturbations in flow distorting the results [20]. Infrared thermography has been used to measure nasal temperature, but this method is restricted to the nasal vestibules and does not provide data on intranasal

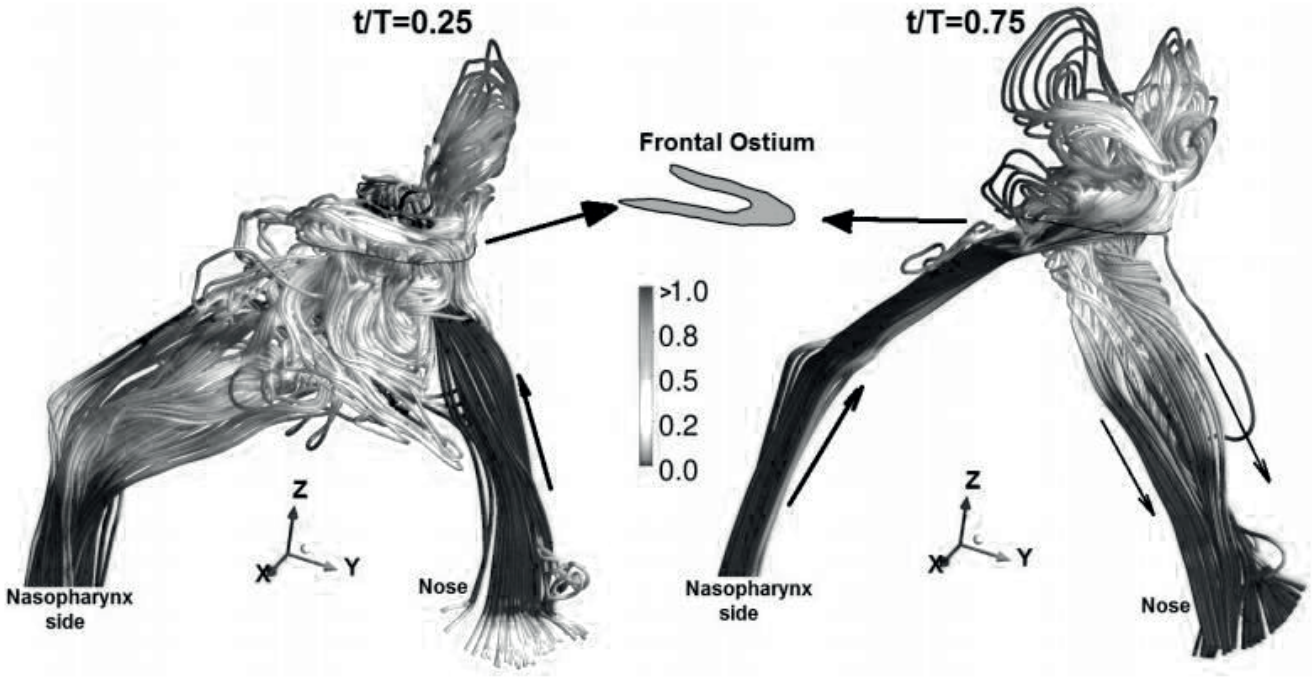

Figure 2. Instantaneous streamline plot at peak inspiration and peak expiration near frontal ostium. Retrieved from Kumar et al. [15].

heating exchanges [43]. Air turbulence is also necessary for efficient air conditioning as it increases contact between airflow and the mucosa, improving the efficiency of heat and humidity exchange during the respiratory cycle [44].

It has been suggested that airway geometry is the key factor in the heat and humidity exchange capability of the nose [45], and CFD can be utilized to simulate these phenomena in 3D models. CFD prediction of air temperature in different regions of the nasal cavity at the end of inspiration has suggested an average of 25°C in nasal vestibule, 29.2°C in the nasal valve and 31.9°C in the nasopharynx [46]. These findings agree with studies using miniaturized thermocouples in 50 volunteers to measure nasal heat exchange [25 (± 2.1)°C, 29.8 (± 2.5)°C and 33.9 (±1.5)°C, respectively] [47].

CFD modelling suggests that the most important regions for thermal exchange and air conditioning during the inhalation are the anterior turbinate regions whereas heat recovery occurs during exhalation covering the posterior area of the middle and inferior turbinate, and the choana [48]. Other CFD models have suggested that air flow heating was more effective at the superior and inferior parts of the nasal cavity. This reflects the passage of 60% of the airflow between the middle and inferior conchae, whereas about 8% flows through the superior aspect of the cavity and about 33% through the inferior aspect, so the airflow has more time to be heated in the upper and lower regions [46].

CFD may also be useful for demonstrating changes in the thermal balance due to nasal pathologies or surgical procedures. Septal perforations in anterior-caudal positions reduced the temperature and humidity of the inhaled air, whereas anterior-cranial and posterior-caudal perforations have minimum impact on these parameters [49]. These results explain why anterior-caudal septal perforations lead to mucosal dehydration, epistaxis, and crusting. CFD models have shown that surgeries for reduction of inferior turbinates can change the nasal airflow pattern and, consequently, reducing heat transfer [50]. Resection of the head of inferior turbinate left the nasal cavity's ability to heat cold air almost unchanged. However, the air temperature in the nasopharynx was 12% lower when the inferior turbinate was partially removed, and 18% lower in radical inferior turbinectomies, comparing to intact nasal cavities.

Regarding the paranasal sinuses, a virtual simulation has demonstrated that increased airflow in the maxillary ostium after endoscopic surgery reduced the temperature at this site and also decreased the absolute humidity by about 9% in the maxillary sinus. A colder, drier postoperative environment may explain why some patients develop recalcitrant crusts and mucus thickening after sinusotomies [34].

Particle deposition

The transnasal route can be used to administer steroids and saline irrigations for local treatments as well as systemic medications such as insulin, oxytocin and growth hormone [51-54]. Howe-

ver, to ensure adequate dosage, topical drugs must be reliably distributed and deposited on the nasal mucosa [55]. The deposition of particles can be influenced by the speed and turbulence of the airflow, the particle size, density and shape, the exposure time of the mucosa to the airstream, and morphological features such as nasal and nostril geometry [45, 56]. However, frequent variations in speed and direction of the airflow in each region of the nasal cavity, along with the physiological characteristics of ciliary movement, mucus and nasal congestion make modelling difficult.

The main challenge is to combine both qualitative and quantitative analysis in a non-invasive method. The addition of dyes or radioisotopes to topical medicines whose distribution is then detected by radiological or scintigraphic scans or endoscopic examination provides information on the topographic distribution of medicines. However, these techniques can be sometimes invasive and are limited by low resolution and/or radiation exposure [57, 58].

CFD models can provide information on the influence of different patterns of nasal anatomy, airflow velocity, particle size, the velocity of the jet, cone diameter and position of the spray in the nostril during application [45, 58]. With this method, it is possible to improve the design and effectiveness of several mechanisms of delivery of medications within the nasal cavity.

One of the most important barriers to the delivery of medications to the nasal cavity is the nasal valve. This region is situated in the anterior part of the nasal airway where there is both the smallest cross-sectional area and the highest resistance to airflow. The particle delivery achieved by 18 different nasal spray devices in different positions has been simulated by CFD, and it was found that only in 15 out 48 spray simulations particles penetrated through the nasal valve and reached the turbinates, septum, and lateral wall [59]. The probability of particles reaching the nasal cavity can be improved in different ways: the reduction of the particle size (20 µm) and spray velocity (1m/sec), by 1 cm of nozzle penetration distance into the nostril, and the presence of gentle inspiratory airflow (15L/min).

Virtual models of particle deposition in possible drug targets, such as the olfactory region, nasal valve and turbinates were performed [24, 52], and showed that most particles released from nasal devices were deposited in the anterior portion of the nose and did not reach the nasal mucosa, limiting the desired therapeutic effect. One of these studies concluded that nasal administration by nebulizers seems to be efficient and reduces the impaction of the particles in the anterior nasal cavity since they generate small particles (10-20 µm) with low-velocity airflow (7.5-15 L / min). Higher spray particles delivered at higher rates may increase drug loss through the nasopharynx [24].

In one CFD study on nanoparticle deposition, two different spray devices (hollow and a solid spray cone) were analysed [16]. When delivering 5 µm particles, both devices had a nasal deposition pattern of about 25%. The same study found almost complete of deposition on the nasal mucosa when nanoparticles (1nm) were delivered in a low flow rate (4L/min), but the deposition was found within the anterior region of the nasal cavity. At a flow rate of 10L/min the delivery was more dispersed throughout the nasal cavity, but with a deposition rate reduced to 40%. It has been found that, for a fixed breathing rate, as the particle size decreased, the total nanoparticle deposition increased, and that total particle deposition declined as the flow rate increased [36].

The study of drug administration is extremely complex and the search for an ideal mechanism can be altered by regional or ethnic factors. CFD modelling has been used to study the different nose and sinus deposition patterns of intranasal sprayed particles in Asian, African American, Latin American and Caucasian subjects with "normal" computed tomography [60]. The computational simulations showed no particle deposition in the maxillary sinuses of all subjects studied, although there was considerable deposition in the osteomeatal complex. For small particle sizes (5 µm – 15 µm), Asians had the most cumulative delivery, while African Americans had greater deposition of sizes particles (20 µm – 50 µm). Caucasians had the fewest localized regions with particle deposition.

Since the peculiar anatomy of the sinuses prevents the passage through their ostia and makes it impossible to insert sensors inside them, CFD has been proved to be a useful tool for simulating and analysing the entry and deposition of particles at these sites [61]. In a CFD model which studied the deposition of three different nanoparticle sizes (1, 10 and 40 nm) within the maxillary sinus, no particle passed through the ostium into the maxillary sinus. SPECT–CT and gamma-scintigraphy have been used to validate these results [62] and found that the deposition in frontal sinuses was nil, and less than 1% of the total particle deposition was detected within the ethmoid and maxillary sinuses.

Patients who fail medical treatment for chronic rhinosinusitis usually need to undergo endoscopic sinus surgery (FESS), a procedure which aims to open the paranasal sinuses and improve mucosal ventilation and mucus clearance. An important goal of this surgery is also to increase the delivery of drugs to the paranasal mucosa. CFD has been used to study the effect of four different sizes of antrostomies on the delivery of different particle sizes into the maxillary sinus [33]. The results showed that the

particles deposition fraction was less than 0.05% in all controls, and the highest nebulised and sprayed deposition was achieved after mega antrostomy. Virtual endoscopic sphenoidotomy has shown an increase of particle deposition in this sinus from 0% to 1.5% [37] and this deposition rose proportionally with particle size until the maximum of 10 µm diameter, then decreased for larger particles (with an airflow between 5 and 7.5 L/min). Similarly, another CFD study found an increase of particle deposition into maxillary sinus after uncinectomy and middle meatal antrostomy, comparing with pre-operative control, with maximum deposition for 10 µm particles [36].

High-volume irrigation is used frequently after sinus surgeries and considered one of the most effective methods of topical drug delivery as it enters the postoperative sinuses more effectively than sprays or nebulizers. To verify the effectiveness of this method in different head positions and flow rates, virtual nasal irrigations have been simulated by using pre- and postoperative computerised tomography scans of endoscopic sinus surgeries (including modified endoscopic Lothrop or Draf III procedures) [63]. The CFD results demonstrated that low-flow irrigation (12 mL/sec) at the head position of 90° was more effective in reaching the preoperative ethmoidal and maxillary sinus, although it did not reach the frontal sinus. After a modified endoscopic Lothrop procedure this sinus was largely filled by irrigation. However, due to the partial removal of the superior septum and frontal intersinus septum in this procedure, the irrigation of the other sinuses was impaired, as irrigation spilt through the interseptal communication and flowed out of the contralateral nostril.

Limitations

Like all methods used for the study of nasal physiology, CFD also has limitations. One of these is related to the time required to perform the simulation. After obtaining the image (TC or RMI) the process of constructing the 3D model and carrying out the simulations involves several days of work. In 2010, Leong et al. [9] described that a personal computer required 28 days to complete a simulation. With the constant evolution of computer power and speed, this time has reduced. However, it is still necessary hours of specialized work to obtain the results of a CFD simulation [14]. In addition, due to exposure to radiation from the CT scan, CFD should be indicated in selected cases, where its results could positively aid medical decisions and therapeutic results. The use of MRI would be a more appropriate alternative, although it is still an expensive and time-consuming examination.

A significant challenge to CFD modelling is the variable geometry of the nasal cavity due to the rhythmic engorgement of the nasal mucosa [23], which may be a determinant of overall nasal resistance as well as modifying the flow in that cavity [20]. Although nasal physiology is extremely dynamic, CFD simulations only provide information from a static moment, portrayed at the time the CT or MRI were performed [14]. Such a feature neglects the mucosal lining of the cavity and considers the limits of the nasal cavity as rigid walls. Nasal physiology also hampers the CFD simulation of particle filtration and intranasal humidification. Although possible, such simulation is difficult to perform accurately because active and dynamic physiological processes such as local blood flow, congestion and active mucus secretion by glands cannot be adequately simulated. The variability of airflow within the entire respiratory cycle is also not considered in the CFD simulations. Changes in pressure and airflow velocity vary constantly within a complete respiratory cycle. As demonstrated by rhinomanometry, neither the pressure nor the airflow velocity is the same at the beginning and end of the inspiratory or expiratory cycle [41].

Another important limitation of CFD is related to the validation of the results obtained. Unlike in engineering, where CFD data can be directly confirmed, such measurements are difficult to obtain in rhinology. The introduction of measurement devices into the nasal cavity can affect the normal respiratory cycle, reducing the reliability of the results. In addition, such devices provide localized measurement, whereas CFD provides a comprehensive analysis of the entire nasal cavity. Recently, other methods have been applied to confirm CFD results such as particle image velocimetry technique [45, 64] and 3D synthetic human-like models [40]. However, although some results are similar to CFD models, as described above, data obtained in synthetic models or cadavers also do not take into account the physiological changes that occur in the nasal cavity during the respiratory cycle. The results of airflow measurements obtained in rhinomanometry have already been compared to those found in the CFD simulations and have shown to be very similar [38]. However, more studies based on the comparison of CFD with the current gold-standard methods for the measurement of nasal physiology, such as acoustic rhinometry and PNIF, would be useful to validate the results of the virtual simulations. Therefore, despite the many advantages of virtual simulations, more studies need to be performed to fully validate the results.

It remains to be seen how the variations of airflow, pressure, humidity, and temperature are related to patients' well-being so that CFD modelling is clinically useful [14]. Several types of research have compared data obtained in CFD before and after surgical treatments. However, few studies have linked such data to postoperative clinical outcomes. Numerical simulations may become a useful tool for surgical planning in the future, but cannot yet predict the clinical results of rhinologic surgeries [41].

Conclusion

CFD is a method of analysis originating from engineering for aerospace and hydraulic studies. This methodology has been adapted for medicine and applied to several fields, including vascular surgery, pneumology and otorhinolaryngology. In rhinology, these numerical simulations have been widely used to evaluate nasal physiology data such as airflow and pressure distribution, as well as heat and moisture exchange. CFD also analyses the effects of anatomical variations such as septal deviations and perforations, turbinate hypertrophy, and the effect of surgery. Virtual models have also been used to analyse the delivery and deposition of medications in the nasal cavity, guiding the development of new techniques and delivery mechanisms. Although it remains an expensive and labour-intensive method, CFD may become a viable diagnostic tool in the future as it has many advantages over conventional methods for studying nasal physiology such as rhinomanometry, acoustic rhinometry and PNIF. However, more studies are needed to validate the results obtained in CFD simulations by comparing them with established methods, and to make this virtual tool faster, less expensive and more applicable to clinical use.

Authorship contribution

SHPL: Data collection, analysis, design, manuscript production;
RJ: Design, analysis, manuscript review;
RGD: Design, analysis, expert manuscript review.

Conflict of interest

The authors have no conflicts of interest or relevant financial interests to disclose.

References

1. Fomin VM, Vetlutsky VN, Ganimedov VL, Muchnaya MI, Shepelenko VN, Melnikov MN, et al. Air flow in the human nasal cavity. (Report). Journal of Applied Mechanics and Technical Physics. 2010;51(2):233.
2. André RF, Vuyk HD, Ahmed A, Graamans K, Nolst Trenité GJ. Correlation between subjective and objective evaluation of the nasal airway. A systematic review of the highest level of evidence. Clinic Otolaryngol. 2009;34(6):518-25.
3. Weinhold I, Mlynski G. Numerical simulation of airflow in the human nose. Eur Arch Otorhinolaryngol. 2004;261(8):452-5.
4. van Egmond MMHT, van Heerbeek N, Ter Haar ELM, Rovers MM. Clinimetric properties of the Glasgow Health Status Inventory, Glasgow Benefit Inventory, Peak Nasal Inspiratory Flow, and 4-Phase Rhinomanometry in adults with nasal obstruction. Rhinology. 2017;55(2):126-34.
5. Parthasarathi K, Christensen JM, Alvarado R, Barham HP, Sacks R, Harvey RJ. Airflow and symptom outcomes between allergic and non-allergic rhinitis patients from turbinoplasty. Rhinology. 2017;55(4):332-8.
6. Moxness MH, Bugten V, Thorstensen WM, Nordgård S, Bruskeland G. A comparison of minimal cross-sectional areas, nasal volumes and peak nasal inspiratory flow between patients with obstructive sleep apnea and healthy controls. Rhinology. 2016;54(4):342-7.
7. Tsounis M, Swart KMA, Georgalas C, Markou K, Menger DJ. The clinical value of peak nasal inspiratory flow, peak oral inspiratory flow, and the nasal patency index. Laryngoscope. 2014;124(12):2665-9.
8. Ottaviano G, Scadding GK, Iacono V, Scarpa B, Martini A, Lund VJ. Peak nasal inspiratory flow and peak expiratory flow. Upright and sitting values in an adult population. Rhinology. 2016;54(2):160-3.
9. Leong SC, Chen X, Lee H, Wang D. A review of the implications of computational fluid dynamic studies on nasal airflow and physiology. Rhinology. 2010;48(2) 139-45.
10. Bailie N, Hanna B, Watterson J, Gallagher G. An overview of numerical modelling of nasal airflow. Rhinology. 2006;44(1):53-7.
11. Mlynski G, Grützenmacher S, Plontke S, Grützmacher W, Mlynski B, Lang C. A method for studying nasal air flow by means of fluid dynamics experiments. Z Med Physik. 2000;10(3):207-14.
12. Keyhani K, Scherer PW, Mozell MM. Numerical simulation of airflow in the human nasal cavity. J biomech eng. 1995;117(4):429.
13. Chen XB, Lee SC, Leong HP, Chong VFH, Wang DY. Aerodynamic effects of inferior turbinate surgery on nasal airflow - A computational fluid dynamics model. Rhinology. 2010;48(4):394-400.
14. Quadrio M, Pipolo C, Corti S, Lenzi R, Messina F, Pesci C, et al. Review of computational fluid dynamics in the assessment of nasal air flow and analysis of its limitations. Eur Arch Otorhinolaryngol. 2014;271(9):2349-54.
15. Kumar H, Jain R, Douglas RG, Tawhai MH. Airflow in the Human Nasal Passage and Sinuses of Chronic Rhinosinusitis Subjects. Pub Lib Sci (PLoS ONE).2016;11(6): e0156379.
16. Ge Q. Numerical studies of fluid-particle dynamics in human respiratory system. Melbourne: RMIT University; 2012.
17. Yu C, Chen S-H, Wang G, Wang Y. Numerical analysis of flow characteristics for the normal human upper airway. Biomed. Eng. Appl. Basis Commun.2016;28(02):1650012.
18. Lee HP, Poh HJ, Chong FH, Wang DY. Changes of airflow pattern in inferior turbinate hypertrophy: a computational fluid dynamics model. Am J rhinol allergy. 2009;23(2):153-58.
19. Tan J, Han D, Wang J, Liu T, Wang T, Zang H, et al. Numerical simulation of normal nasal cavity airflow in Chinese adult: a computational flow dynamics model. Eur Arch Otorhinolaryngol. 2012;269(3):881-89.
20. Doorly DJ, Taylor DJ, Schroter RC. Mechanics of airflow in the human nasal airways. Resp Physio Neurob. 2008;163(1):100-10.
21. Chen XB, Lee HP, Chong VFH, Wang DY. Impact of inferior turbinate hypertrophy on the aerodynamic pattern and physiological functions of the turbulent airflow - a CFD simulation model. Rhinology. 2010;48(2):163-8.
22. de Gabory L, Reville N, Baux Y, Boisson N, Bordenave L. Numerical simulation of two consecutive nasal respiratory cycles: toward a better understanding of nasal physiology. Int Forum Allergy Rhinol. 2018;XX:1-10.
23. Zhao K, Jiang J. What is normal nasal airflow? A computational study of 22 healthy adults. Int Forum Allergy Rhinol. 2014;4(6):435-46.
24. Schroeter JD, Kimbell JS, Asgharian B. Analysis of particle deposition in the turbinate and olfactory regions using a human nasal computational fluid dynamics model. J Aerosol Med. 2006;19(3):301-13.
25. Chen XB, Lee HP, Hin Chong VF, Wang DY. Assessment of septal deviation effects on nasal air flow: A computational fluid dynamics model. Laryngoscope. 2009;119(9):1730-6.
26. Garcia GJM, Kimbell JS, Rhee JS, Senior BA. Septal deviation and nasal resistance: An investigation using virtual surgery and computational fluid dynamics. Am J Rhinol Allergy. 2010;24(1):e46-e53.
27. Garcia GJM. Visualization of nasal airflow patterns in a patient affected with atrophic rhinitis using particle image velocimetry. J Physics: Conference Series. 2007;85(1):012032-7.
28. Lindemann J, Brambs HJ, Keck T, Wiesmiller KM, Rettinger G, Pless D. Numerical simulation of intranasal airflow after radical sinus surgery. Am J Otolaryngol Head Neck Med Surg. 2005;26(3):175-80.
29. Lee KB, Jeon YS, Chung SK, Kim SK. Effects of partial middle turbinectomy with vary-

ing resection volume and location on nasal functions and airflow characteristics by CFD. Comput Biol Med. 2016;77:214-21.
30. Ozlugedik S, Nakiboglu G, Sert C, Elhan A, Tonuk E, Akyar S, et al. Numerical Study of the Aerodynamic Effects of Septoplasty and Partial Lateral Turbinectomy. Laryngoscope. 2008;118(2):330-4.
31. Na Y, Chung KS, Chung SK, Kim SK. Effects of single-sided inferior turbinectomy on nasal function and airflow characteristics. Respir Physiol Neurobiol. 2012;180(2-3):289-97.
32. Simmen D, Sommer F, Briner H, Jones N, Kroger R, Hoffmann T, et al. The effect of Pyriform Turbinoplasty on nasal airflow using a virtual model. Rhinology. 2015;53(3):242-8.
33. Wofford MR, Kimbell JS, Frank-Ito DO, Dhandha V, McKinney KA, Fleischman GM, et al. A computational study of functional endoscopic sinus surgery and maxillary sinus drug delivery. Rhinology. 2015;53(1):41-8.
34. Jain R, Kumar H, Tawhai M, Douglas R. The impact of endoscopic sinus surgery on paranasal physiology in simulated sinus cavities. Int Forum Allergy Rhinol. 2017;7(3):248-55.
35. Frank DO, Zanation AM, Dhandha VH, McKinney KA, Fleischman GM, Ebert CS, et al. Quantification of airflow into the maxillary sinuses before and after functional endoscopic sinus surgery. Int Forum Allergy Rhinol. 2013;3(10):834-40.
36. Abouali O, Keshavarzian E, Farhadi Ghalati P, Faramarzi A, Ahmadi G, Bagheri MH. Micro and nanoparticle deposition in human nasal passage pre and post virtual maxillary sinus endoscopic surgery. Respir Physiol Neurobiol. 2012;181(3):335-45.
37. Bahmanzadeh H, Abouali O, Faramarzi M, Ahmadi G. Numerical simulation of airflow and micro-particle deposition in human nasal airway pre- and post-virtual sphenoidotomy surgery. Comput Biol Med. 2015;61:8-18.
38. Zachow S, Muigg P, Hildebrandt T, Doleisch H, Hege HC. Visual Exploration of Nasal Airflow. IEEE Trans Visual Comput Graph. 2009;15(6):1407-14.
39. Doorly D, Taylor DJ, Franke P, Schroter RC. Experimental investigation of nasal airflow. J Engin Med. 2008;222(4):439-53.
40. Kook Kim J, Yoon JH, Hoon Kim C, Wook Nam T, Bo Shim D, Ae Shin H. Particle image velocimetry measurements for the study of nasal airflow. Acta Otolaryngol. 2006;126(3):282-7.
41. Keck T, Lindemann J. Numerical simulation and nasal air-conditioning. GMS Curr Top Otolaryngol Head Neck Surg. 2010;9:Doc08. PMC.Web.20 nov 2017.
42. Lindemann J, Leiacker R, Rettinger G, Keck T. Nasal mucosal temperature during respiration. Clin Otolaryngol. 2002;27(3):135-9.
43. Kastl KG, Wiesmiller KM, Lindemann J. Dynamic infrared thermography of the nasal vestibules: A new method. Rhinology. 2009;47(1):89-92.
44. Noback ML, Harvati K, Spoor F. Climate-related variation of the human nasal cavity. Am J Physic Anthropol. 2011;145(4):599-614.
45. Inthavong K. Simulation of fluid dynamics and particle transport in a realistic human nasal cavity. Melbourne: RMIT University; 2008.
46. Yu S, Sun X, Liu Y. Numerical analysis of the relationship between nasal structure and its function. Sci World J. 2014;14:1-6.
47. Keck T, Leiacker R, Riechelmann H, Rettinger G. Temperature Profile in the Nasal Cavity. Laryngoscope. 2000;110(4):651-4.
48. Castro F, Parra T, Quispe C, Castro P. Numerical simulation of the performance of a human nasal cavity. Eng Comp. 2011;28(6):638-53.
49. Lindemann J, Reichert M, Kroger R, Schuler P, Hoffmann T, Sommer F. Numerical simulation of humidification and heating during inspiration in nose models with three different located septal perforations. Eur Arch Otorhinolaryngol. 2016;273(7):1795-800.
50. Chen X, Lee H, Chong V, Wang D. Numerical simulation of the effects of inferior turbinate surgery on nasal airway heating capacity. Am J Rhinol Allergy. 2010;24(5):E118-E22.
51. Heinemann L. New ways of insulin delivery. Int J Clinic Prac. 2011;65:31-46.
52. Frank DO, Kimbell JS, Cannon D, Pawar SS, Rhee JS. Deviated nasal septum hinders intranasal sprays: A computer simulation study. Rhinology. 2012;50(3):311-18.
53. Leitner VM, Guggi D, Krauland AH, Bernkop-Schnürch A. Nasal delivery of human growth hormone: in vitro and in vivo evaluation of a thiomer/glutathione microparticulate delivery system. J Contr Release. 2004;100(1):87-95.
54. Guastella AJ, Ward PB, Hickie IB, Shahrestani S, Hodge MAR, Scott EM, et al. A single dose of oxytocin nasal spray improves higher-order social cognition in schizophrenia. Schizophrenia Research. 2015;168(3):628-33.
55. Albu S. Novel drug-delivery systems for patients with chronic rhinosinusitis. Drug Des Dev Ther. 2012;6:125-32.
56. Heyder J, Rudolf G. Mathematical models of particle deposition in the human respiratory tract. J Aerosol Sci. 1984;15(6):697-707.
57. Aggarwal R, Cardozo A, Homer J. The assessment of topical nasal drugdistribution. Clinic Otolaryngol. 2004;29(3):201-5.
58. Chen X, Lee H, Chong V, Wang D. Drug delivery in the nasal cavity after functional endoscopic sinus surgery: a computational fluid dynamics study. J Laryngol Otol. 2012;126(5):487-94.
59. Kimbell JS, Segal RA, Asgharian B, Wong BA, Schroeter JD, Southall JP, et al. Characterization of deposition from nasal spray devices using a computational fluid dynamics model of the human nasal passages. J aerosol med. 2007;20(1):59-74.
60. Keeler JA, Patki A, Woodard CR, Frank-Ito DO. A Computational Study of Nasal Spray Deposition Pattern in Four Ethnic Groups. J Aerosol Med Pulm Drug Deliv. 2016;29(2):153-66.
61. Na Y, Kim K, Kim SK, Chung S-K. The quantitative effect of an accessory ostium on ventilation of the maxillary sinus. Resp Physiol Neurobiol. 2012;181(1):62-73.
62. Leclerc L, Pourchez J, Prevot N, Vecellio L, Le Guellec S, Cottier M, et al. Assessing sinus aerosol deposition: Benefits of SPECT-CT imaging. Int J Pharma. 2014;462(1-2):135-41.
63. Zhao K, Craig Jr, Cohen N, Adappa N, Khalili S, Palmer J. Sinus irrigations before and after surgery. Visualization through computational fluid dynamics simulations. Laryngoscope. 2016;126(3):E90-E6.
64. Inthavong K, Tian ZF, Tu JY, Yang W, Xue C. Optimising nasal spray parameters for efficient drug delivery using computational fluid dynamics. Comput Biol Med. 2008;38(6):713-26.

Richard Douglas
Department of Surgery
The University of Auckland
Private Bag 92019
Auckland 1142
New Zealand

Tel: +64 9 373 7599 ext 89820
Fax: +64 9 377 9656
E-mail:
richard.douglas@auckland.ac.nz